

## New Spin-Transition-Like Copper(II)–Nitroxide Species

Catherine Hirel,<sup>†</sup> Licun Li,<sup>†</sup> Peter Brough,<sup>†</sup> Kira Vostrikova,<sup>‡</sup> Jacques Pécaut,<sup>†</sup> Boubker Mehdaoui,<sup>§</sup> Maxime Bernard,<sup>§</sup> Philippe Turek,<sup>§</sup> and Paul Rey<sup>\*†</sup>

CEA-Grenoble, Département de Recherche Fondamentale sur la Matière Condensée, Service de Chimie Inorganique et Biologique (UMR-E3, CEA-UJF), 17 rue des Martyrs F38054 Grenoble Cedex 09, France, Laboratory of Cluster Chemistry and Supramolecular Assemblies, Institute of Inorganic Chemistry, 3 Lavrentiev. Avenue, 630090 Novosibirsk, Russia, and Institut de Chimie (UMR 7177, CNRS-ULP), 1 rue Blaise Pascal, BP 296 R8, 67008 Strasbourg Cedex, France

Received May 10, 2007

Novel copper(II)–nitroxide complexes exhibiting a spin-transition-like behavior have been prepared and characterized. They include meso, chiral, and racemic 2-(3-pyridyl)-nitronyl nitroxides differently substituted in positions 4 and/or 5 by ethyl groups and pyrimidyl nitroxides. Depending on the stoichiometry of the reaction, tetranuclear and binuclear complexes were obtained whose structures are cyclic. The tetranuclear species, which include two intracyclic and two exocyclic metal sites, are similar to the previously reported complex of the tetramethylated analogue, while the binuclear complexes involve only endocyclic metal ions and have uncoordinated N-oxyl groups. The tetranuclear complexes exist as two isomers depending on the temperature of crystallization: at room temperature, N-oxyl ligand coordination is axial–axial, while it is axial–equatorial at low temperature. Unexpectedly, this isomerism concerns N-oxyl bonding to the exocyclic metal centers for the derivatives of 4,5-diethyl-substituted ligands while it involves the endocyclic metal site in the complex of the monoethylated ligand, which converts reversibly from a high-spin state to a low-spin state, as observed for the complex of the tetramethylated ligand. Binuclear complexes are diamagnetic at room temperature but convert to a paramagnetic state on warming (90–110 °C); the transition is irreversible and sharp.

## Introduction

Organic free radicals are now widely used as spin carriers in magnetochemistry.<sup>1</sup> Those that have a delocalized structure, such as nitronyl nitroxides free radicals,<sup>2</sup> are particularly attracting because numerous coupling pathways favor the

onset of bulk magnetic properties in the solid state.<sup>3</sup> However, the popularity of nitronyl nitroxides mainly stems from their coordination properties.<sup>4</sup> Their metal complexes are characterized by strong direct exchange couplings between organic and metal unpaired electrons and properties highly dependent on the structure of the free radical and on the nature of the metal ion.

Among all magnetic materials built from nitronyl nitroxides, spin-transition-like species are particularly interesting. They are copper(II) complexes built from nitroxides substituted by a nitrogen-containing group which cannot function as a chelating ligand (Scheme 1) such as 3-pyridyl and 4-pyrrazolyl groups.<sup>5</sup>

\* To whom correspondence should be addressed. E-mail: paul.rey@cea.fr.

<sup>†</sup> Service de Chimie Inorganique et Biologique.

<sup>‡</sup> Institute of Inorganic Chemistry.

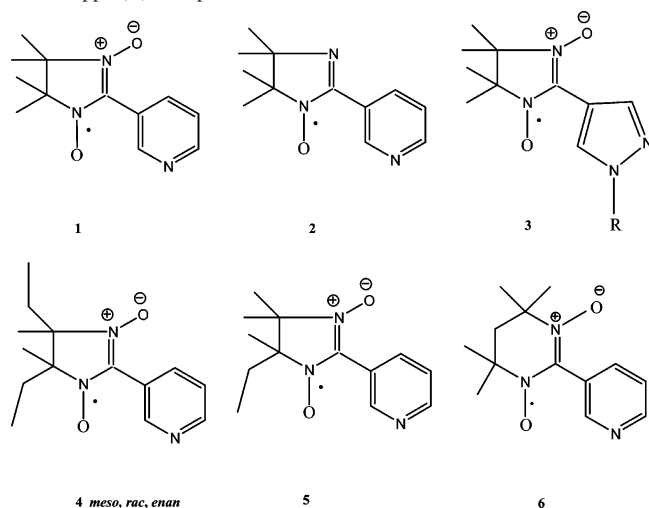
<sup>§</sup> Institut de Chimie.

- (1) For reviews, see: (a) Ovcharenko, V. I.; Sagdeev, R. Z. *Usp. Khim.* **1999**, *68*, 381–400; *Russ. Chem. Rev.* **1999**, *68*, 345–363. (b) *Magnetism: A Supramolecular Function*; Kahn, O., Ed.; Kluwer Academic: Dordrecht, 1996. (c) *Mol. Cryst. Liq. Cryst.* **1997**, *305/306*, 1–586–1–520. (d) *Mol. Cryst. Liq. Cryst.* **1999**, *334/335*, 1–712–1–706. (e) *Magnetic Properties of Organic Materials*; Lahti, P. M., Ed.; Marcel Dekker: New York 1999. (f) *Molecular Magnetism*; Itoh, K.; Kinoshita, M., Eds.; Gordon and Breach: Amsterdam, 2000. (g) Amabilino, D. B.; Veciana J. In *magnetism: Molecules to Materials II*; Miller, J. S., Drillon, M., Eds.; Wiley-VCH: Weinheim, 2000; p 1.
- (2) (a) Osiecki, J. H.; Ullman, E. F. *J. Am. Chem. Soc.* **1968**, *90*, 1078. (b) Ullman, E. F.; Call, L.; Osiecki, J. H. *J. Org. Chem.* **1970**, *35*, 3623. (c) Ullman, E. F.; Osiecki, J. H.; Boocock, D. G. B.; Darcy, R. *J. Am. Chem. Soc.* **1972**, *94*, 7049. (d) Hirel, C.; Vostrikova, K. E.; Ovcharenko, V. I.; Pécaut, J.; Rey, P. *Chem. Eur. J.* **2001**, *7*, 2007.

(3) Kinoshita, M.; Turek, P.; Tamura, M.; Nozawa, K.; Shiomi, D.; Nakazawa, Y.; Ishikawa, M.; Takahashi, M.; Awaga, K.; Inaba, T.; Maruyama, Y. *Chem. Lett.* **1991**, *7*, 1225.

(4) (a) Caneschi, A.; Gatteschi, D.; Sessoli, R.; Rey, P. *Acc. Chem. Res.* **1989**, *22*, 392. (b) Caneschi, A.; Gatteschi, D.; Rey, P. *Progr. Inorg. Chem.* **1991**, *39*, 331.

(5) Rey, P.; Ovcharenko V. I. In *magnetism: Molecules to Materials IV*; Miller, J. S., Drillon, M., Eds.; Wiley-VCH: Weinheim, 2003; p 41, and references therein.

**Scheme 1.** Nitroxide Ligands Used in the Design of Spin-Transition-Like Copper(II) Complexes

The first reported example of such a compound was a cyclic centrosymmetric tetranuclear complex built from  $\text{Cu}(\text{hfac})_2$  and **1** which converted reversibly (100–110 K) without hysteresis from a high-spin state ( $S = 6 \times 1/2$ ) to a low-spin state ( $S = 2 \times 1/2$ ) on decreasing the temperature.<sup>6</sup> This conversion corresponds to a change of coordination of a oxyl oxygen from axial to equatorial within the coordination sphere of the endocyclic metal ion inducing a change of magnetic interaction from weakly ferromagnetic to strongly antiferromagnetic. The imino nitroxide analogue **2** led to a similar complex exhibiting a transition at a different temperature (70–80 K), which is reversible and displays hysteresis ( $\Delta T = 12$  K).<sup>7</sup>

Recent progress in this field was recently achieved using **3**, in which the 4-pyrrazolyl fragment also includes a nonchelating nitrogen coordination site; copper(II) complexes of this ligand are linear polynuclear species.<sup>8–11</sup> Different derivatives have been characterized depending on a head-to-head or a head-to-tail attachment to the metal ions.<sup>8</sup> Depending also on the R substituent, several spin-transition-like behaviors have been observed—different transition temperatures, presence or not of hysteresis—and more importantly, a few compounds exhibited a high-spin state at low temperature.<sup>9</sup> This behavior has been elegantly explained showing that copper(II)–nitroxide species might be more versatile species than conventional metal-based spin-transition complexes.

Although these features are attractive, they show up at rather low temperatures and we examined possibilities to

increase the conversion temperature. Since spin pairing at low temperature is associated to N-oxyl equatorial coordination, it was anticipated that steric crowding might have a strong influence on the occurrence of the process. Indeed, change of coordination from axial to equatorial, which results in a shorter metal–O(oxyl) distance, should appear at higher temperature when steric hindrance around the donor atom increases. Along this line, we undertook a study aimed at investigating the effect of N(oxyl) steric crowding on the characteristics of the transition. Three different types of ligands were considered (**4–6**), which are shown in Scheme 1, and arranged in order of supposed decreasing steric demand. Type 1 (**4**) carries two ethyl groups in positions 4 and 5 of the imidazoline ring and exists in three forms, meso, enantiopure, and racemic.<sup>12</sup> In addition to steric crowding resulting from the presence of ethyl groups, **4meso** and **4rac** are suitable to give, like **1**, cyclic centrosymmetric complexes while **4enan** (*S*(+) or *R*(-)) might lead to extended structures since the molecule should be acentric. Type 2, (**5**) only available as the racemic mixture, carries only one ethyl group in position 4 (or 5) and, thus, two unequivalent coordinating oxyl groups, a feature which may result in isomeric complexes having different properties. Finally, type 3, (**6**) a pyrimidyl nitronyl nitroxides, has been shown to have oxyl groups more sterically crowded than imidazolynyl analogues due to a larger N–C–N angle.<sup>13</sup>

In the following are reported the synthesis, structural characterization, and magnetic properties of  $\text{Cu}(\text{hfac})_2$  derivatives of these ligands. It is shown that steric crowding has strong and unexpected influence on the structure and properties of the complexes and that the transition temperature can be varied in this way.

## Experimental Section

Solvents were purified according to standard literature methods. Reagents were used as received from Aldrich. The ESR spectra were recorded in dilute deoxygenated solution using a Bruker EMX spectrometer operating at X-band frequency. Solid-state EPR was performed with an ESP300E spectrometer (Bruker) operating at X-band and equipped with a continuous-flow cryostat (ESR 900, Oxford) for temperature control down to liquid helium. <sup>1</sup>H NMR spectra were determined at ambient temperature using a Bruker AC200 (with the deuterated solvent as the lock and tetramethylsilane as the internal reference). Magnetic susceptibility data were recorded using a Quantum Design SQUID magnetometer. Elemental analyses were determined by the CNRS, Service Central d'Analyse, Département d'Analyse Élémentaire. The UV–vis spectra were obtained using a HP 8453 single-beam spectrometer. X-ray crystallography was carried out on a Bruker AXS using a CCD detector and SMART diffractometer.

**Syntheses.** **4meso**, **4rac**, and **4enan**, 2-(3-pyridyl)-4,5-diethyl-4,5-dimethylimidazolynyl-3-oxide-1-oxy, and 2-(3-pyridyl)-4,4,6,6-tetramethylpyrimidyl-3-oxide-1-oxy (**6**) were prepared as described elsewhere.<sup>12,13</sup>

- (6) Lanfranc de Panthou, F.; Belorizky, E.; Calemzuk, R.; Luneau, D.; Marcenat, C.; Ressoche, E.; Turek, P.; Rey, P. *J. Am. Chem. Soc.* **1995**, *117*, 11247.  
 (7) Lanfranc de Panthou, F.; Luneau, D.; Musin, R.; Ohmström, L.; Grand, A.; Turek, P.; Rey, P. *Inorg. Chem.* **1996**, *35*, 3484.  
 (8) Fokin, S.; Ovcharenko, V.; Romanenko, G.; Ikorskii, V. *Inorg. Chem.* **2004**, *43*, 969.  
 (9) Ovcharenko, V. I.; Fokin, S. V.; Romanenko, G. V.; Shvedenkov, Yu. G.; Ikorskii, V. N.; Tretyakov, E. V.; Vasilevsky, S. F.; Sagdeev, R. *Z. Mol. Phys.* **2002**, *100*, 1107.  
 (10) Ovcharenko, V. I.; Fokin, S. V.; Romanenko, G. V.; Shvedenkov, Yu. G.; Ikorskii, V. N.; Tretyakov, E. V.; Vasilevsky, S. F. *Russ. J. Struct. Chem.* **2002**, *43*, 153.  
 (11) Maryunina, K.; Fokin, S.; Ovcharenko, V.; Romanenko, G.; Ikorskii, V. *Polyhedron* **2005**, *24*, 2094.

- (12) Hirel, C.; Pécaut, J.; Choua, S.; Turek, P.; Amabilino, D. B.; Veciana, J.; Rey, P. *Eur. J. Org. Chem.* **2005**, 348.  
 (13) Brough, P.; Pécaut, J.; Rassat, A.; Rey, P. *Chem. Eur. J.* **2006**, *12*, 5134.

**rac-2,3-Dimethyl-2,3-dinitropentane.**<sup>14–16</sup> Lithium (0.760 g, 0.110 mol) was added to absolute methanol (15 mL) cooled in an ice bath. When the metal was consumed, the solvent was removed under vacuum to give LiOCH<sub>3</sub> as a white solid, which was dispersed in 200 mL of dry DMSO. Then, 2-nitropropane (10 g, 0.112 mol) was added and the mixture stirred at room temperature for 2 h. 2,2-Dinitrobutane (8.0 g, 0.054 mol), prepared according to a published procedure,<sup>15</sup> was then added portionwise. After being stirred at room temperature for an additional 6 h, 1.5 L of H<sub>2</sub>O was carefully added and the white precipitate which formed was immediately filtered. This precipitate was dissolved in diethyl ether and the solution dried over Na<sub>2</sub>SO<sub>4</sub>. After evaporation of the solvent, 8.5 g (83%, mp 88 °C) of *rac*-2,3-dimethyl-2,3-dinitropentane was obtained and used as such in the following steps. Anal. Calcd for C<sub>7</sub>H<sub>14</sub>N<sub>2</sub>O<sub>4</sub>: C, 44.21; H, 7.34; N, 14.74. Found: C, 44.38; H, 7.27; N, 14.82.

**rac-2-(3-Pyridyl)-4,4,5-trimethyl-5-ethylimidazolyl-3-oxide-1-oxy (5).** To 4.75 g (25 mmol) of *rac*-2,3-dimethyl-2,3-dinitropentane in a 1:1 mixture of water and THF (50 mL) was added ammonium chloride (2.5 g). Zinc powder (10 g) was added portionwise to this mixture cooled to 10 °C during 45 min. The slurry was then stirred for an additional 1 h. After filtration, the precipitate was washed with water (4 × 25 mL). To the combined filtrate and washings was added 2.7 g (25 mmol) of 3-pyridinecarboxaldehyde, and the mixture was stirred at room temperature for 4 h. After filtration, 3.0 g of *rac*-1,3-dihydroxy-2-(3-pyridyl)-4,4,5-trimethyl-5-ethylimidazole were obtained as a pale yellow solid, which was not further characterized.

To 3 g (16 mmol) of this compound in CH<sub>2</sub>Cl<sub>2</sub> (300 mL) cooled in an ice bath was added NaIO<sub>4</sub> (5.5 g) dissolved in water (50 mL), and the mixture was stirred for 0.5 h. The organic phase was separated, dried (Na<sub>2</sub>SO<sub>4</sub>), and concentrated to give a dark blue solid, which was chromatographed on Al<sub>2</sub>O<sub>3</sub> (III) with diethyl ether as eluent to give 1.2 g (41%, mp = 75–76 °C) of **5** as a deep blue solid. Anal. Calcd for C<sub>13</sub>H<sub>18</sub>N<sub>3</sub>O<sub>2</sub>: C, 62.88; H, 7.31; N, 16.92. Found: C, 63.14; H, 7.44; N, 17.03. Single crystals suitable for a X-ray diffraction study were grown by slow evaporation of a solution of the radical in hexane-diethyl ether (1:1) at room temperature.

**{[Cu(hfac)<sub>2</sub>](L)<sub>2</sub>} (7).** Cu(hfac)<sub>2</sub> (100 mg, 0.21 mmol) was dissolved in heptane (30 mL) at 50 °C. A solution of **L** (0.5 mmol) in CH<sub>2</sub>Cl<sub>2</sub> (5 mL) was added to give a microcrystalline blue precipitate, which was filtered and dried. The filtrate was allowed to stand at ambient temperature for slow evaporation, and deep blue single crystals were obtained after 5 days. All compounds analyzed satisfactorily for C, H, N, and Cu.

**{[Cu(hfac)<sub>2</sub>]<sub>2</sub>(L)<sub>2</sub>} (9–12).** A typical procedure is as follows for **11**. A solution of Cu(hfac)<sub>2</sub> (143 mg, 0.3 mmol) in heptane (30 mL) was warmed to 50 °C. A solution of **5** (38 mg, 0.15 mmol) in 3 mL of CH<sub>2</sub>Cl<sub>2</sub> was added and the resulting solution was stirred for 5 min at 50 °C, cooled to room temperature, and kept in the dark at 4 °C. After 3 days, red-brown crystals (60 mg, 55%, mp = 106 °C) were collected. Anal. Calcd for **11**, C<sub>33</sub>H<sub>22</sub>N<sub>3</sub>O<sub>10</sub>F<sub>24</sub>Cu<sub>2</sub>: C, 32.92; H, 1.83; N, 3.49; Cu, 10.56. Found: C, 33.29; H, 1.79; N, 3.43; Cu, 10.63. **9meso** (63%, mp = 109 °C); **9rac** (57%, mp = 89 °C); **9enan** (71%, mp = 82 °C); **12** (77%, mp = 127 °C). If crystallization occurs at 20 °C, green complexes are obtained:

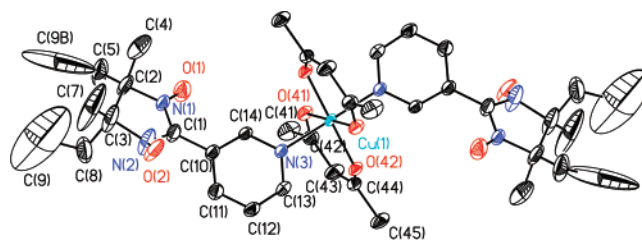


**Figure 1.** Molecular structure of **7meso**, [(Cu(hfac)<sub>2</sub>)(**4meso**)<sub>2</sub>]. Thermal ellipsoids are drawn at the 30% probability level. Fluorine and hydrogen atoms are not represented.

**10meso** (59%, mp = 117 °C); **10rac** (46%, mp = 101 °C); **10enan** (38%, mp = 96 °C).

**[Cu(hfac)<sub>2</sub>(L)<sub>2</sub>] (13–14).** To a solution of Cu(hfac)<sub>2</sub> (143 mg, 0.30 mmol) in warm (50 °C) heptane (30 mL) was added with stirring a solution of **5** (76 mg, 0.32 mmol) in CH<sub>2</sub>Cl<sub>2</sub> (5 mL). A blue precipitate immediately was produced. The resulting mixture was stirred for an additional 5 min and cooled to room temperature, and the blue powder (110 mg, 65%, mp = 110 °C) was collected by filtration. Slow evaporation of the filtrate at room temperature produced blue needle crystals of **14** after 1 week. Anal. Calcd for **14**, C<sub>23</sub>H<sub>20</sub>N<sub>3</sub>O<sub>6</sub>F<sub>12</sub>Cu: C, 38.05; H, 2.78; N, 5.79; Cu, 8.76. Found: C, 38.29; H, 2.79; N, 5.83; Cu, 8.63. **13meso** (76%, mp = 110 °C); **13rac** (23%, mp = 149 °C); **13enan** (38%, mp = 102 °C).

## Results and Discussion

**Syntheses and Structural Properties.** The preparation of ligand **5** needs no comment since it followed well-established procedures derived from Ullman's work.<sup>2</sup>

The syntheses of the copper(II) complexes were performed in heptane according to previously reported recipes varying the relative proportions of Cu(hfac)<sub>2</sub> and ligand.<sup>4,6</sup> In all cases, blue species having a high melting point (ca 200 °C), which as found for **1**,<sup>17,18</sup> are obtained when 2 mol of ligand were used for 1 mol of Cu precursor. They correspond to the coordination of two ligands by their pyridyl nitrogen and oxyl groups are not involved as coordination sites. These species have not been fully characterized for all ligands because metal–ligand interactions are weak and their magnetic behaviors follow Curie laws down to low temperature. As an example, the molecular structure of **7meso** [(Cu(hfac)<sub>2</sub>)(**4meso**)<sub>2</sub>] is displayed in Figure 1.

Changing the stoichiometry afforded several other complexes. For nitroxides **4**, expected to have the most sterically crowded oxyl groups, the stoichiometry was changed for two metal ions to one ligand leading to tetranuclear clusters in which the three potentially (O, O, N) coordinating sites of the ligands are active and whose structures are cyclic like that of **8** ({[Cu(hfac)<sub>2</sub>]<sub>2</sub>(**1**)<sub>2</sub>}).<sup>6</sup> Surprisingly, however, depending on the temperature of crystallization, two isomeric complexes of each ligand were obtained which were easily recognized as different species because **9**, crystallized at 4 °C, is red-brown while the other, **10**, was obtained at 20 °C and is green. The study of these species was complicated by a slow transformation in the solid state of

(14) Kornblum, N.; Singh, H. K.; Kelly, W. J. *J. Org. Chem.* **1983**, *48*, 332.

(15) Rueppel, M. L.; Rapoport, H. *J. Am. Chem. Soc.* **1970**, *92*, 5783.

(16) Kornblum, N.; Boyd, S. D.; Stuchal, F. W. *J. Am. Chem. Soc.* **1970**, *92*, 5784.

(17) Lanfranc de Panthou, F. Ph. D. Thesis, Grenoble 1994.

(18) Ma, Y.; Gao, D.-Z.; Zhang, W.; Yoshimura, K.; Liao, D.-Z.; Jiang, Z.; Yan, S.-P. *Inorg. Chim. Acta* **2006**, *359*, 4655.

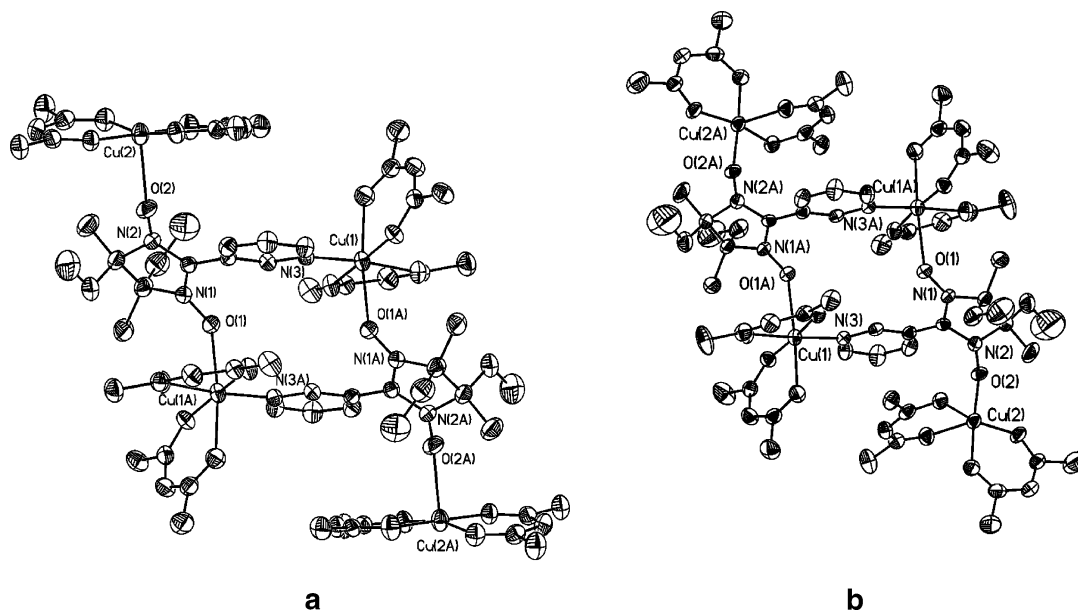


**Figure 2.** Molecular structure of  $\{[\text{Cu}(\text{hfac})_2]_2(\mathbf{4rac})\}_2$ , (a) **10rac**, red-brown, (b) **9rac**, green. Hydrogen and fluorine atoms are not represented.

the green species into the brown ones at room temperature at a speed depending on the ligand. This feature resulted in unstable single crystals for some green derivatives; moreover, we were unable to grow single crystals of the complexes of the enantiopure ligands (**4enan**). However, both modifications of the *rac* ligand (**9rac** and **10rac**) were fully characterized and, with the help of the magnetic properties, it was possible to get a clear picture of the species for which single crystals were not available.

The complexes derived from **4rac** are shown in Figure 2.

Like that of **8**, these structures both exhibit a centrosymmetric cyclic binuclear core and two pending pentacoordinated metal sites. In the cyclic fragment, the pyridyl nitrogen of each ligand is equatorially bound to an octahedral metal ion whose coordination sphere is completed by a cis-coordinated oxyl oxygen in the axial position ( $\text{Cu}-\text{O} = 2.570(4)$  and  $2.466(4)$  Å for **9rac** and **10rac**, respectively) belonging to the other ligand. The two pending square-pyramidal  $\text{Cu}(\text{hfac})_2$  fragments are linked to the second oxyl group of each ligand. The only significant, but most important, difference stems from an equatorial coordination of the oxyl group to the pending metal fragment in **9rac** ( $1.955(4)$  Å) while it is axial in **10rac** ( $2.344(3)$  Å). Considering the numerous reports devoted to  $\text{Cu}$ -nitroxide derivatives,<sup>4,19–24</sup> it was expected that at least one equatorially coordinated oxyl group giving rise to a strong charge-transfer band was present in the red-brown species (**9rac**) while, in

the green complexes, all oxyl groups were axially linked. Note that the slow transformation of the green species into the red-brown one corresponds to a switch from axial to equatorial of the  $\text{Cu}-\text{O}(\text{oxyl})$  bond in the pending metal fragment. In this respect, the conversion (a change from axial to equatorial) is similar to that observed in **8** except that in the latter the change of coordination takes place in the cyclic core and involves the octahedral metal site.<sup>6</sup> However, the conversion **10**  $\rightarrow$  **9** is so slow that one could hardly consider this phenomenon as a spin transition; note that the reverse transformation from red-brown to green was never observed on heating.

Using the same stoichiometry, similar structural arrangements, **11** (green) and **12** (red-brown), were obtained from **5** and **6**, respectively, and only one complex was characterized in each case independently of the temperature of crystallization; both **11** and **12** were stable at room temperature, and in particular, no color change was observed. Note that **11** displays a bis-axial coordination pattern as that observed in all green species (**10**) and in the analogue involving **1** (**8**, high-temperature structure) while in **12** the arrangement is axial–equatorial-like in red-brown complexes (**9**). In the latter, coordination to the endocyclic metal occurs with a surprisingly long bond ( $>2.6$  Å) while the other oxyl group is equatorially bound. One could expect that axial–axial coordination would help in releasing steric hindrance, but this complex is stable up to the melting point and is obtained even if the solvent (heptane) is evaporated at  $100$  °C.

Finally, a 1:1 stoichiometry afforded other metal–nitroxide red-brown derivatives (**13**–**14**) that are binuclear species exhibiting a cyclic molecular structure where the oxyl group is equatorially bound to the metal (Figure 3).

Note that **13enan**, derived from **4enan** (the enantiopure ligand), is not an extended linear compound; it crystallizes in a chiral space group ( $P2_12_12_1$ ) and exhibits a noncentrosymmetric cyclic molecular structure. Worthy of note, on

- (19) Tretyakov, E.; Fokin, S.; Romanenko, G.; Ikorskii, V.; Vasilevsky, S.; Ovcharenko, V. *Inorg. Chem.* **2006**, *45*, 3671.  
 (20) Rajadurai, C.; Falk, K.; Ostrovsky, S.; Enkelmann, V.; Haase, W.; Baumgarten, M. *Inorg. Chim. Acta* **2005**, *358*, 3391.  
 (21) Caneschi, A.; Gatteschi, D.; Grand, A.; Laugier, J.; Pardi, L.; Rey, P. *Inorg. Chem.* **1988**, *27*, 1031.  
 (22) Musin, R. N.; Schastnev, P. V.; Malinovskaya, S. A. *Inorg. Chem.* **1992**, *31*, 4118.  
 (23) Caneschi, A.; Gatteschi, D.; Laugier, J.; Rey, P. *J. Am. Chem. Soc.* **1987**, *109*, 2191.  
 (24) Caneschi, A.; Gatteschi, D.; Hoffman, S. K.; Laugier, J.; Rey, P.; Sessoli, R. *Inorg. Chem.* **1988**, *27*, 2390.

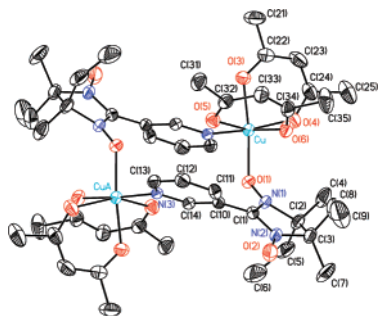


**Figure 3.** Molecular structure of compound **13rac** showing the atom-labeling scheme. Ellipsoids are drawn at the 30% probability level; fluorine and hydrogen atoms are not represented.

heating (when measuring the melting point for example) **13meso**, **13rac**, and **14** changed to green before melting.

Meaningful bond distances and angles for structurally characterized complexes are reported in Table 1.

On examining Table 1, one sees that in all tetranuclear species the intracyclic metal center is axially oxyl-bound while, contrastingly, in all binuclear compounds, the metal–ligand coordination is equatorial. In compound **11**, the presence of only one ethyl group in the ligand (**5**) brings some steric release but the ligation to the intracyclic metal ion is still axial through the less-crowded oxyl group located close to the carbon atom which carries two methyl groups. In the binuclear complex (**14**) of the same ligand, however, coordination to the metal center occurs with the other oxyl group, which is close to the carbon atom bearing the ethyl substituent and is probably the more hindered. It is not clear whether the oxyl group close to the ethyl substituent is more basic and if this effect is strong enough to overcome steric crowding. All attempts to characterize other species derived from this ligand failed. Considering the steric demand of the different ligands, no clear relation with the coordination pattern emerges. Nitronyl nitroxides are stable only if the carbon atoms (positions 4 and 5)  $\alpha$  to the oxyl groups are fully substituted, a feature responsible for oxyl steric crowding even in the familiar tetramethylated radicals. However, they function as  $\mu_{1,3}$ -bridging ligands toward most metal ions even if bulky ancillary ligands such as hexafluoroacetylacetonato are present.<sup>4</sup> Considering copper(II), the situation is complicated by the fact that coordination may occur as equatorial with a short bond or as axial with a long bond and the metal may adopt different coordination patterns, octahedral or square pyramidal. Although a few nitroxides carrying a small substituent (Me, Et) are  $\mu_{1,3}$ -bridging in a bis-axial fashion,<sup>23</sup> when the substituent is more sterically demanding, complexes with  $\text{Cu}(\text{hfac})_2$  are trinuclear species where only the central metal ion is hexacoordinate while two terminal metal sites are pentacoordinate.<sup>24</sup> A similar situation is observed in the complexes under study, which may be viewed as dimers of two similar fragments ( $\text{Cu1}-\text{ON}-\text{NO}-\text{Cu2}$ ). On examining the  $\text{Cu1}-\text{Cu2}$  distance, one sees that the metal ions are, as expected, slightly closer in red-brown derivatives (axial–equatorial coordination pattern, **9** and **12**) than in green compounds (**10** and **11**) where both oxyl groups are axially coordinated. On comparing the two

forms **9rac** and **10rac** of the same ligand **4rac**, one observes, however, a similar  $\text{Cu1}-\text{Cu2}$  distance (8.056(6) vs 8.045(5) Å) because axial bonding to the endocyclic metal site in **10** is shorter than in **9**.

The most interesting feature of this structural study stems from the fact that at low temperature (vide supra for **11**) all species carry one equatorial ligation to the metal, in agreement with an earlier suggestion that spin pairing is probably a stabilizing factor.<sup>5</sup> It is indeed worthy of note that between the two isomers obtained for the diethyl substituted ligands (**9**, **10**), the red-brown one including an equatorial bonding is obtained at low temperature and is probably the thermodynamically stable species. The “axial–axial” compound appears to be kinetically controlled; it is obtained because it crystallizes better even if it is the less-stable form.

**Magnetic Properties.** Magneto-structural correlations in copper(II)–nitroxide complexes are well established.<sup>4,17–24</sup> Equatorial coordination of the oxyl group results in strong antiferromagnetic metal–radical interactions, while in axial-coordinated species, where the magnetic orbitals are quasi-orthogonal but the  $\text{Cu}-\text{oxyl}$  bond is long, the coupling is weakly ferromagnetic.

Following these crude rules, the observed magnetic behavior of the tetranuclear complexes is straightforwardly understood. The red-brown species (**9** and **12**) where one oxyl ligation is equatorial all exhibit a Curie behavior ( $\chi T = 0.85 \text{ cm}^3 \text{ K mol}^{-1}$ ) corresponding to two independent  $1/2$  spins ( $g > 2$ ). Spin-pairing between the radicals and the pending metal ions results in the “disappearance” of four spins so that one observes, even at room temperature, only the two intracyclic  $\text{Cu(II)}$  ions to which the nitroxide is axially bound. For the green species (**10**), measurement of the magnetic data was complicated by the presence of red-brown impurities leading to  $\chi T$  values at room temperature always weaker (ca.  $2 \text{ cm}^3 \text{ K mol}^{-1}$ ) than that expected for six independent  $1/2$  spins ( $2.25 \text{ cm}^3 \text{ K mol}^{-1}$  if  $g = 2$ ) and depending on the age of the sample. Qualitatively, however,  $\chi T$  vs  $T$  agrees with the rules mentioned before since it increases smoothly on decreasing the temperature showing that, indeed, ferromagnetic interactions are operative. Attempts to figure out these coupling constants were unsuccessful, owing to the presence of red-brown impurities and because it was impossible to discriminate the coupling pathways within the cyclic fragment.

One green compound (**11**) however, has a specific magnetic behavior displayed in Figure 4.

The values of  $\chi T$  at room temperature ( $2.5 \text{ cm}^3 \text{ K mol}^{-1}$ ) and at 2 K ( $0.88 \text{ cm}^3 \text{ K mol}^{-1}$ ) correspond well to six and to two independent  $1/2$  spins, respectively ( $g > 2$ ). This conversion from a high-spin state to a low-spin state on decreasing the temperature occurs without observable hysteresis and, in this respect, is similar to that observed for the homologous complex involving **1** (**8**).<sup>6</sup> However, comparing these two spin-transition-like behaviors, one observes a displacement of the transition from  $T_{1/2} = 110 \text{ K}$  in **8** to  $T_{1/2} = 163 \text{ K}$  in **11**. Note also that the conversion is spread over a larger temperature range in **11**. These two compounds

**Table 1.** Selected Structural Bond Lengths (Å) and Angles (deg) for the Cu(II) Complexes<sup>a</sup>

	Cu1–O1	Cu1–N3	Cu2–O2	N1–O1	N2–O2	Cu1–Cu2	N1–O1–Cu1	N2–O2–Cu2
<b>8 (300 K)</b>	2.384(7)	2.022(6)	2.316(8)	1.251(10)	1.308(10)		122.9(4)	
<b>(50 K)</b>	2.028(50)	2.052(30)	2.404(36)					
<b>9meso</b>	2.548(4)	2.031(5)	1.964(4)	1.275(6)	1.327(6)	7.983(7)	128.4(5)	119.1(6)
<b>9rac</b>	2.553(4)	2.034(4)	1.955(4)	1.277(6)	1.285(5)	8.056(6)	130.3(4)	120.5(3)
<b>9enan</b>	–	–	–	–	–	–	–	–
<b>10meso</b>	–	–	–	–	–	–	–	–
<b>10rac</b>	2.466(4)	2.028(3)	2.344(3)	1.285(3)	1.283(3)	8.045(5)	134.9(5)	147.3(5)
<b>10enan</b>	–	–	–	–	–	–	–	–
<b>11</b>	2.401(3)	2.020(3)	2.320(4)	1.280(4)	1.284(5)	8.184(5)	124.0(2)	133.0(3)
<b>12</b>	2.659(5)	2.022(4)	1.969(4)	1.275(5)	1.315(5)	7.472(7)	129.9(5)	124.2((3)
<b>13meso</b>	–	–	–	–	–	–	–	–
<b>13rac</b>	1.969(3)	1.994(3)	–	1.308(4)	1.270(4)	–	123.8(2)	–
<b>13enan</b>	1.968(2)	1.992(2)	–	1.306(3)	1.266(3)	–	124.5(1)	–
	1.976(2)	1.992(2)	–	1.312(2)	1.263(3)	–	123.2(1)	–
<b>14</b>	1.985(7)	1.993(9)	–	1.28(1)	1.27(1)	–	124.0(7)	–

<sup>a</sup> Cu1 and Cu2 are endocyclic and pending metal sites, respectively. Compound **8** ( $\{[Cu(hfac)_2]_2(\mathbf{1})\}_2$ ) has been included for comparison.<sup>6</sup>

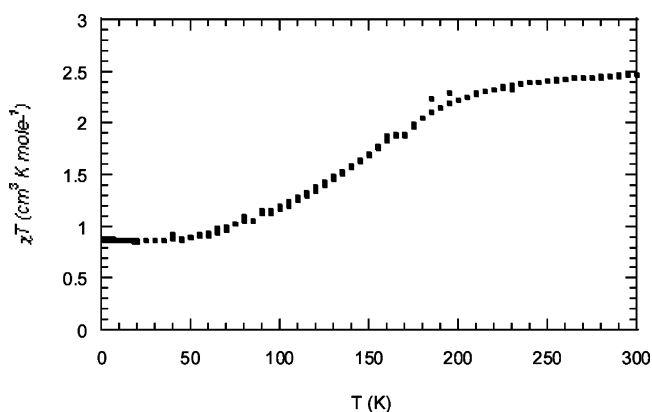


**Figure 4.** Magnetic behavior of complex **11** in the form of  $\chi T$  vs  $T$ . The data were recorded at a 0.5 T field strength, and the temperature was varied from 300 to 2 K and back from 2 to 300 K.

(**8** and **11**) have similar room-temperature structures, and probably, conversion from a high-spin to a low-spin state involves a switch from axial to equatorial of the oxyl coordination to the *endocyclic* metal ions. Attempts to confirm this assumption by a low-temperature structural study failed because crystals broke at low temperature.

To sustain this proposal, an EPR study has been performed on powders and crystals of **11** to be compared to previous reports on **8**.<sup>6</sup> It was shown indeed that the EPR response could complete that of the macroscopic static magnetic measurements, yielding an insight in the local magnetic properties. For instance, the EPR of single crystals of **8** just showed isolated  $S = 1/2$  Cu(II) ions below the spin crossover transition. According to the low-temperature structural studies, this feature was straightforwardly ascribed to the exocyclic Cu(II) ions, the endocyclic ones being EPR silent as a result of strong antiferromagnetic coupling with the nitroxide ligands. The present study of the EPR properties of powders of both compounds shows very similar features. A very broad EPR line is observed at room temperature for powders (Figure 5a,b). A very weak Cu(II) single-ion-like signal is superimposed to this broad line which probably corresponds to an uncoupled impurity.

Below the transition, i.e.,  $T = 110$  K for **8**, the EPR signal of an isolated Cu(II) ion in an axial environment is observed

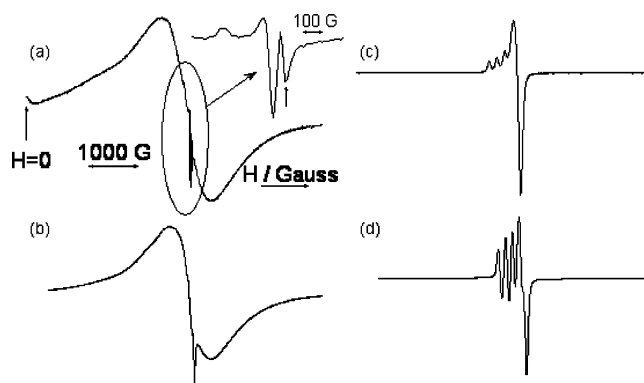


**Figure 5.** EPR spectra at X-band for powder samples of complexes **8** (upper traces) and **11** (lower traces): (a, b) room temperature; (c)  $T = 90$  K; (d)  $T = 140$  K. The inset in (a) shows a magnification of the central line, i.e., the signal of the Cu(II) impurity. An arrow in inset (a) points to a radical impurity centered at  $g = 2.01$  to the right of the Cu(II) line. All spectra have the same field scale as indicated in (a).

with the same symmetry for the hyperfine  $a$  tensor (<sup>63,65</sup>Cu:  $I = 3/2$ ) and the  $g$  tensor,  $g_{\parallel} = 2.31$  and  $g_{\perp} = 2.07$ ;  $a = 156$  G) (Figure 5c). The perpendicular component of the hyperfine tensor is not resolved. It is worth noting that the isolated Cu(II) signal suddenly appears as the main component of the EPR response below the transition for **8**. This is not the case for **11**, where a similar study shows that a similar signal does superimpose progressively to the broad component from ca. 160 K, being the solely observed EPR spectrum below 140 K, with similar  $g$  tensor and  $a$  tensor as for **8** but with axial compression, i.e.,  $g_{\perp} = 2.27$  and  $g_{\parallel} = 2.07$ ,  $a_{\perp} = 154$  G (Figure 5d). The observation of well-defined hyperfine splitting rules out any appreciable exchange interaction between these Cu(II) ions and the environment, although this may take place at lower temperature. Therefore, these Cu(II) ions behave as independent and isolated at low temperature, as observed for the exocyclic Cu(II) in **8**. The fact that the transition actually takes place at 160 K, being of the same type in **8** and **11**, is further supported by, e.g., the EPR  $\chi T$  vs  $T$  plot or the plot of the temperature dependence of the average  $g$  factor (Figure 6).

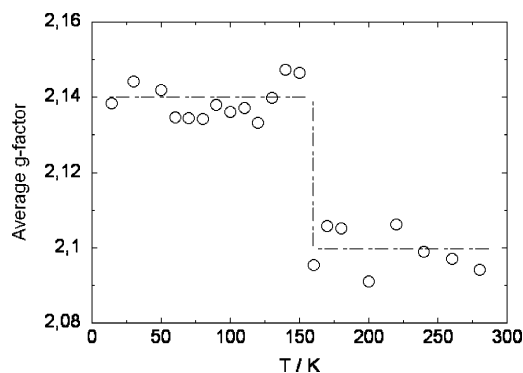


**Figure 6.** Temperature dependence of the average  $g$  factor for the EPR signal of complex **11**. The dash-dotted line is a guide for the eyes.

This corroborates the determination of the transition temperature at half transition  $T_{1/2} = 163$  K from SQUID measurements: the transition actually takes place close to 160 K. The study of the anisotropy of the EPR response of a crystal of **11** at 4 K definitely shows that the  $g$  tensor and the  $a$  tensor of the low-temperature signal are of axial symmetry with the same principal axes. Therefore, we may conclude that the origin of the spin-crossover transition is the same in compounds **8** and **11**, i.e., being a structural change in the coordination geometry from axial to equatorial, with the concomitant change in the magnetic exchange from weak ferromagnetic to strong antiferromagnetic. The main difference originates from a Jahn–Teller-like distortion resulting in an axial compression,<sup>25</sup> which flips the principal axes of the  $g$  and  $a$  tensor of the exocyclic Cu(II) ions in **11** compared to **8**. Furthermore, we may discuss the apparent difference in the shape of the transition for the  $\chi T$  product as revealed by the SQUID measurements, from fairly sharp for **8** to smooth for **11**. The EPR response points to a stronger interplay of the magnetic coupling between the different magnetic species, i.e., endocyclic Cu–radical pairs and extracyclic isolated Cu, in **11** than in **8** with a shift toward higher transition temperature, 160 instead of 110 K. This is exemplified by the overlapping spectra of these magnetic species above the transition temperature in **11** as compared to **8**. This is further supported by a study of the low-temperature EPR signal for both compounds. Extra lines with respect to the main isolated Cu(II)-like line are observed as side features of the EPR spectrum below ca. 14 K in **11**, which are not observed in **8**. The occurrence of a “forbidden”  $\Delta M_s = 2$  half-field line is worth being mentioned. This rich but complex EPR signature cannot be analyzed as resulting solely from, e.g.,  $S = 1$  pairs or other simple spin clusters which could be formed from the 6 spin systems. It is inferred that inter “6 spin-clusters” magnetic interactions occur in complex **11** that do not exist or are too weak to be observed in complex **8**.

As expected for equatorially bound copper–nitroxide species, all binuclear complexes **13**–**14** are spin-paired and diamagnetic at room temperature (Figure 7). On increasing the temperature, one observed a sharp transition to four

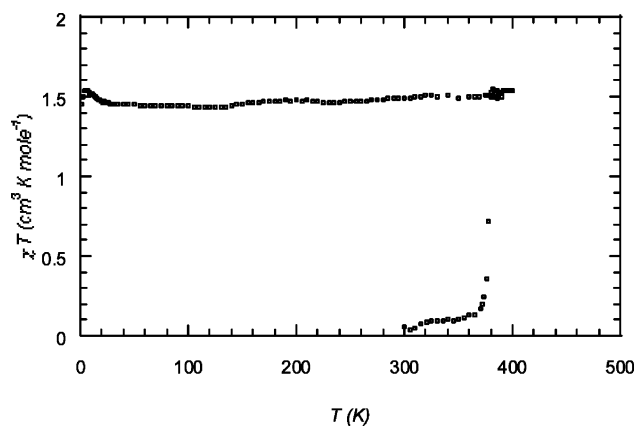


**Figure 7.** Magnetic behavior of **13rac** in the form of  $\chi T$  vs  $T$  in a field of 0.5 T. The temperature was varied from 300 to 400 K and back from 400 to 2 K.

independent spins ( $\chi T = 1.5$  cm<sup>3</sup> K mol<sup>-1</sup>), which occurs at 102, 108, and 89 °C for **13meso**, **13rac**, and **14**, respectively; **13enan** melted before transitioning. These temperatures are strongly correlated with a change of color from red-brown to green already mentioned, as shown by examining the process with a microscope. The transition is *irreversible*. It is interesting to note that at very low temperature,  $\chi T$  increases weakly showing that, probably, copper–nitroxide pairs are weakly ferromagnetically coupled. This fact suggests that, as observed for all transiting species, this conversion is the result of a change of coordination from equatorial to axial.

## Conclusion

This study documents the complexity of Cu(hfac)<sub>2</sub>–nitronyl nitroxide chemistry. In the tetranuclear species, whatever the steric demand of the ligand, at *high temperature* the oxyl group always coordinates in axial position to the octahedral endocyclic metal center, as observed for the tetramethylated ligand. At *low temperature*, in the derivatives of the diethyl-substituted imidazolynyl (**4**) and tetramethyl-substituted pyrimidyl (**6**) ligands, one observes an equatorial coordination of the second oxyl group to the less-crowded square-pyramidal metal ion. In the complex of the pyrimidyl nitroxide, equatorial coordination appears to be strongly stabilized, while in the ethyl-substituted ligands, the difference of energy between the two forms is probably weak. In contrast, for imidazolynyl nitroxide ligands, when the number of ethyl substituents is equal to one (**5**) or zero (**1**), axial–axial binding is observed at room temperature but, at low temperature, equatorial coordination involves the endocyclic octahedral metal site. This behavior is not well understood, but these two complex (**8**, **11**) exhibit structural features in agreement with this finding: examination of Table 1 shows that in all complexes axial coordination occurs with Cu–O–N angles close to 130°, except in **8** and **11** where this angle is in the range expected for equatorial coordination (ca. 120°). Therefore, in these two complexes, change of coordination at the endocyclic metal site may occur with minimum rearrangement of the metal coordination sphere. Indeed, both **8** and **11** exhibit a reversible spin-transition behavior.

(25) Kokoszka, G. F.; Baranowski, J.; Goldstein, C.; Orsini, J.; Mighell, A. D.; Himes, V. L.; Siedle, A. R., *J. Am. Chem. Soc.* **1983**, *105*, 5627.

In the binuclear complexes where steric problems are less acute, N-oxyl coordination is always equatorial at room temperature, resulting in a nonmagnetic ground spin state. The high-temperature coordination is probably axial for these species to convert to a magnetic state corresponding to four independent spins  $S = 1/2$ . Although the transition is irreversible, the domain of temperature (90–110 °C) in which it occurs brings attractiveness to built bistable copper–nitroxide-based compounds.

**Acknowledgment.** P.B. gratefully acknowledges financial support from the Région Rhône-Alpes.

**Supporting Information Available:** X-ray crystallographic files of compounds **7meso**, **9meso**, **9rac**, **10rac**, **11**, **12**, **13rac**, **13enan**, and **14** in cif format. This material is available free of charge via the Internet at <http://pubs.acs.org>.

IC700851X